JACS
JOURNAL OF THE AMERICAN CHEMICAL SOCIETY

Communication

pubs.acs.org/JACS

Determining Charge Transport Pathways through Single Porphyrin Molecules Using Scanning Tunneling Microscopy Break Junctions

Zhihai Li and Eric Borguet*

Department of Chemistry, Temple University, Philadelphia, Pennsylvania 19122, United States

Supporting Information

ABSTRACT: Charge transport in a porphyrin with four identical pyridyl substituents, 5,10,15,20-tetra(4-pyridyl)-21*H*,23*H*-porphine (TPyP), was investigated using the scanning tunneling microscopy break junction method. To determine the dominant pathway, we studied two structurally similar porphyrins, *o*-DPyP and *p*-DPyP. Our experiments reveal that charge transport through TPyP in a break junction configuration does not follow the traditional assumption, i.e., the shortest path between the neighboring side groups. Instead, the charge transport pathway was dominated by the farthest anchoring groups. Furthermore, these single molecule experiments can distinguish between the two structural isomers, which is important in molecular discrimination, porphyrin chemistry, and molecular electronics.

The detailed study of charge transport through individual molecules is important in understanding many chemical and biological reactions and represents a central theme in molecule-based devices.[1−5] As a class of ubiquitous molecules in nature, porphyrins are involved in a wide variety of important biological process, e.g., photosynthesis and biocatalysis. The unique structure and function of porphyrins make them a particular promising system for studying charge transport mechanism[6] and fabricating molecule-based devices to mimic their functionality in nature.[7] Recent technological developments allow measurement of electron transport through objects down to the single molecule level using mechanical controllable break junction (MCBJ)[8−11] or scanning tunneling microscopy (STM) break junctions.[9,12−16] In a break junction experiment, individual molecules are wired between two electrodes by introducing proper anchoring groups, making it possible to measure single molecule conductance (SMC). Though thiols (−SH) are frequently used as anchoring groups, due to the formation of a robust Au−S bond,[17−19] a recent trend is to use linker groups which have weaker coupling with gold electrodes, such as amines,[20,21] pyridyls,[11,21] and isocyanos,[22] as they can form molecular junctions with less fluctuation in conductance due to the reduced variability in binding geometries.[4,20,22,23]

Previous SMC studies focused on molecules with two anchoring groups; multiple anchoring or charge transport pathways have not been explored. In this Communication, we investigate charge transport in a porphyrin with four identical pyridyl substituents, 5,10,15,20-tetra(4-pyridyl)-21*H*,23*H*-porphine (TPyP), using the STM break junction method (Scheme 1). Our experiments reveal that charge transport through a TPyP-mediated junction does not follow the traditionally assumed route, i.e., along the shortest path between the neighboring side groups (Scheme 1B). Instead, the maximum observed in the current histogram may merely reflect the greater probability of the "para" configuration versus the "ortho" one when both are possible (Scheme 1A), which is evidenced by the larger conductance of 5,10-di(4-pyridyl)-15,20-diphenylporphyrin (*o*-DPyP) in comparison with 5,15-di(4-pyridyl)-10,20-diphenylporphyrin (*p*-DPyP).

Scheme 1. Charge Transport Pathways through a Single TPyP Molecule Bridged between Two Electrodes in an STM Break Junction: (A) Through the Farthest Anchoring Groups at the "Para" Positions and (B) Through the Shortest Path between Neighboring Anchoring Groups at the "Ortho" Positions

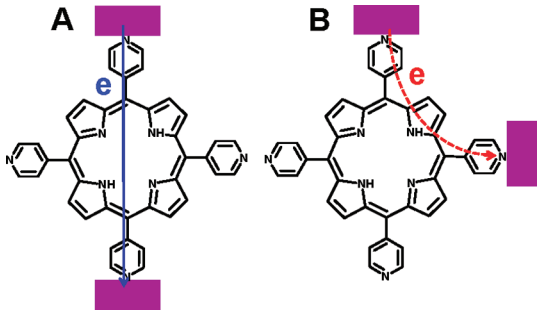

First, we investigated the SMC of TPyP with four identical pyridyl anchor groups, so that charge transport can take place between the pyridyls in either the "para" or "ortho" position of the TPyP. We assumed that the charge transport would predominantly proceed along the shortest path between the neighboring anchoring groups, i.e., along the groups at the "ortho" positions. The details of the sample preparation and STM break junction experiment are described in the Supporting Information (SI). Under these assembly conditions, TPyP adsorbs flat on Au surfaces.[2,24−26] In a break junction experiment, an STM tip is brought into and out of contact with a molecule-modified electrode to repeatedly form molecular junctions while current−distance traces are recorded. The displacement of two electrodes (an STM tip and a substrate) without molecules bridging between them gives rise to quasi-exponentially decaying traces with some noise due to

Received: September 12, 2011
Published: December 1, 2011

 © 2011 American Chemical Society dx.doi.org/10.1021/ja208600v | *J. Am. Chem.Soc.* 2012, 134, 63−66

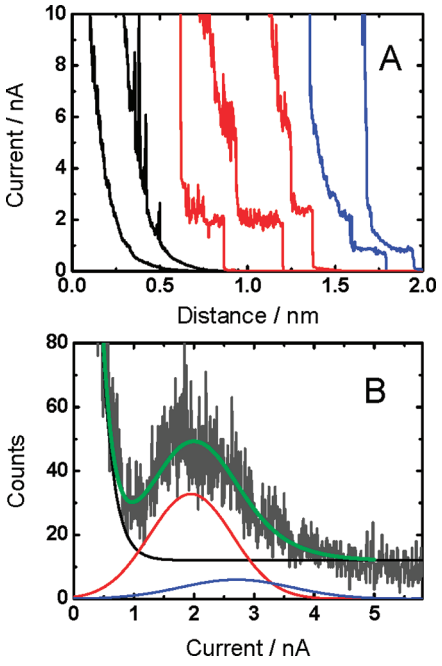

Figure 1. (A) Sample current−distance traces of TPyP in break junction experiments: monotonic decay (black) and stepped curves at V_{bias} = 0.10 V (red) and 0.05 V (blue). (B) Current histogram (dark gray) and fit of the histogram (green) with a function consisting of a gaussian using parameters from a fit for *p*-DPyP (red) and a gaussian using parameters from a fit for *o*-DPyP (blue) and an exponential (black).

instabilities[27] (Figure 1A, black). When molecules are trapped between two electrodes during the stretching of molecular junctions, a current plateau or current step appears in the traces before the current drops.[5] For instance, the current plateaus at ∼2 nA (Figure 1A, red) represent one molecule bridged between two electrodes, and the plateaus with higher current values could be due to multiple molecules trapped in the junction.[5] The plateau current decreased when the bias voltage between electrodes was changed from 0.1 V (Figure 1A, red) to 0.05 V (Figure 1A, blue).

To determine the conductance of single TPyP molecules, we recorded thousands of current-distance traces for statistical analysis. The current histogram in Figure 1B was constructed using 133 stepped traces from 1000 total traces. It shows a current maximum at ∼2.0 nA at a bias voltage of 0.1 V, corresponding to a SMC of 20 nS ($2.58 \times 10^{-4} G_o$; G_o is the quantum of conductance and is equal to 77 500 nS). The current maxima at different biases determined from the corresponding histograms were plotted as a function of bias (SI Figure S1B). The current versus bias plots are quite linear, and the slope of the linear fitting yields molecular conductance of 20.5 ± 2.8 nS, which is consistent with the conductance value from individual traces and histograms (Figure 1).

As there are two possible charge transport pathways in a TPyP molecule with four linker groups (Scheme 1), we could expect to see different peaks in the current histogram. The fact that we observed only one peak indicates either that the two charge transport pathways give the same or similar conductance values or that one of the pathways dominates transport. In order to determine the dominant pathway of charge transport and whether there is a difference between the conductance values of the two possible pathways, we used two other pophyrins that possess only two pyridyl anchoring groups at either the "para" position, 5,15-di(4-pyridyl)-10,20-diphenyl-

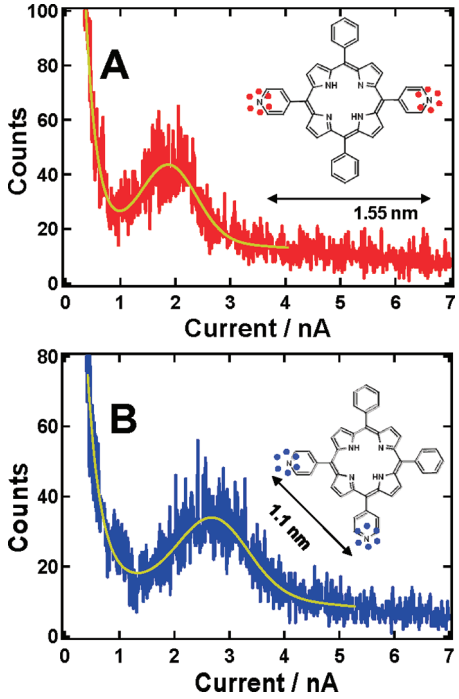

Figure 2. (A) Current histogram of *p*-DPyP constructed from 97 current−distance traces out of 1000 total traces and fitted by a gaussian plus exponential function as a guide to the eye (yellow curve). Inset: molecular structure of *p*-DPyP. (B) Current histogram of *o*-DPyP constructed from 103 current distance traces out of 1000 total traces and fitted by a gaussian plus exponential function as a guide to the eye (yellow curve). Inset: molecular structure of *o*-DPyP.

porphyrin (*p*-DPyP, Figure 2A, inset), or the "ortho" position, 5,10-di(4-pyridyl)-15,20-diphenylporphyrin (*o*-DPyP, Figure 2B, inset). The break junction experiment for these two isomers was performed in the same way as for TPyP. Examples of individual current−distance responses are shown in SI for *p*-DPyP and *o*-DPyP. The histograms constructed from all stepped traces show a current maximum of ∼1.95 nA for *p*-DPyP, almost equal to the current maximum for TPyP, and ∼2.7 nA for *o*-DPyP. The current peaks in the histograms (Figure 2) can be determined by the gaussian plus exponential fittings (see details in SI) to be 1.97 and 2.75 nA, corresponding to a SMC of 19.7 and 27.5 nS for *p*-DPyP and *o*-DPyP, respectively, when the bias voltage is equal to 0.10 V. The difference in the conductance of *p*-DPyP and *o*-DPyP shows that structurally similar isomers (*p*-DPyP and *o*-DPyP) can be distinguished with break junction techniques by measuring and comparing their SMC. There is no evidence for direct connection of the tip to the porphyrin ring, which would have resulted in identical conductances for *o*-DPyP and *p*-DPyP.

Surprisingly, the conductance of a single TPyP is very close to the conductance of *p*-DPyP, which has a longer charge transport pathway. In other words, these observations reveal that charge transport in a TPyP-mediated STM break junction does not proceed along the shortest pathway between anchoring groups, i.e., the anchoring groups at the "ortho" positions. Instead, the charge transport pathway through TPyP was dominated by the farthest anchoring groups located at the

dx.doi.org/10.1021/ja208600v | *J. Am. Chem.Soc.* 2012, 134, 63−66

"para" positions, which is evidenced by the similarity of the conductance of *p*-DPyP and TPyP, 19.7 and 20.5 nS, respectively. In comparison, the conductance of *o*-DPyP, 27.5 nS, is much greater. Tentatively, we ascribe this observation to the contact geometry of TPyP in molecular junctions (SI Figure S4). When the STM tip lifts a TPyP molecule from the surface by pulling on one anchoring group, the most stable geometry appears to be that with two anchoring group at the "para" positions connected to the two electrodes (an STM tip and a substrate). For instance, at the initial stage of pulling a TPyP molecule, when one pyridyl group makes contact with the STM tip, it is possible that all other pyridyls are in contact with the substrate. Further pulling will lift either one or both pyridyls at the "ortho" positions with respect to the pyridyl connected to the STM tip. Lifting two pyridyls, at one the "ortho" position and one at the "para" position, simultaneously and leaving another *o*-pyridyl anchored on a substrate (Figure S4C) appears not to be a stable configuration. Instead, the most probable configuration for a TPyP in a stretching junction involves the two groups at the farthest positions in contact with two electrodes (Figure S4B).

This interpretation also can explain the observation of a high conductance peak (27.5 nS) for *o*-DPyP, but not in the TPyP experiments. The absence of two peaks in the histogram for TPyP may reflect the greater stability of the "para" connection compared to the "ortho" connection, and the fact that when these two connections are possible TPyP favors the "para" connection in the junction. The assumption was well supported by fitting the current histogram of TPyP (Figure 1B) with a function consisting of a gaussian for a "para" connection, using parameters from a fit for *p*-DPyP (Figure 1B, red), and a gaussian for an "ortho" connection, using parameters from a fit for *o*-DPyP (Figure 1B, blue) and an exponential (Figure 1B, black). The fitting equation, parameters, and details are listed in the SI, showing that the overwhelming contribution to the current histogram of TPyP comes from "para"-connected junctions (~80%), further supporting the conclusion that electron transport through the "para" positions is the dominating pathway.

In summary, we have demonstrated that the charge transport pathway through a tailored porphyrin can be determined by the STM break junction technique. Our experiments reveal that charge transport through TPyP-mediated junctions does not follow the traditional assumption: the shortest path between the neighboring anchoring groups should be the most probable charge transport path. Instead, the detailed analysis shows that electron transport through "para" positions is more probable, possibly due to the greater stability of the "para" connection compared to the "ortho" connection. Thus, when both connections are possible, TPyP favors the "para" connection in the junction. Furthermore, these experiments show that single molecule charge transport can distinguish between two porphyrin isomers of identical mass and chemical formula. The ability to reveal the charge transport pathway at the single molecule level and further distinguish between the two structural isomers as demonstrated in this paper may provide insight into the charge transport mechanisms, molecular discrimination, the design of molecule-based devices and porphyrin chemistry.

■ ASSOCIATED CONTENT

Supporting Information

Experimental details, conductance versus bias voltage, current−distance traces for *p*-DPyP and *o*-DPyP, and influence of different fittings on molecular conductance. This material is available free of charge via the Internet at http://pubs.acs.org.

■ AUTHOR INFORMATION

Corresponding Author

eborguet@temple.edu

■ ACKNOWLEDGMENTS

We thank Dr. Yangjun Xing, Aashish Tuladhar, and Asghar Razavi for help with the software for statistical analysis and fitting of SMC data. Financial support from the National Science Foundation (CHE 0809838) is gratefully acknowledged.

■ REFERENCES

(1) Nitzan, A.; Ratner, M. A. *Science* **2003**, *300*, 1384−1389.
(2) Sedghi, G.; Sawada, K.; Esdaile, L. J.; Hoffmann, M.; Anderson, H. L.; Bethell, D.; Haiss, W.; Higgins, S. J.; Nichols, R. J. *J. Am. Chem. Soc.* **2008**, *130*, 8582−8583.
(3) Choi, S. H.; Kim, B.; Frisbie, C. D. *Science* **2008**, *320*, 1482−1486.
(4) Mishchenko, A.; Zotti, L. A.; Vonlanthen, D.; Burkle, M.; Pauly, F.; Cuevas, J. C.; Mayor, M.; Wandlowski, T. *J. Am. Chem. Soc.* **2011**, *133*, 184−187.
(5) Xu, B. Q.; Tao, N. J. *Science* **2003**, *301*, 1221−1223.
(6) Sedghi, G.; García-Suárez, V. M.; Esdaile, L. J.; Anderson, H. L.; Lambert, C. J.; Martin, S.; Bethell, D.; Higgins, S. J.; Elliott, M.; Bennett, N.; Macdonald, J. E.; Nichols, R. J. *Nature Nanotechnol.* **2011**, *6*, 517−523.
(7) Higgins, S. J.; Nichols, R. J. *Nature Nanotechnol.* **2007**, *2*, 270−271.
(8) Kim, Y.; Song, H.; Strigl, F.; Pernau, H. F.; Lee, T.; Scheer, E. *Phys. Rev. Lett.* **2011**, *106*, 196804.
(9) Song, H.; Reed, M. A.; Lee, T. *Adv. Mater.* **2011**, *23*, 1583−1608.
(10) van der Molen, S. J.; Liljeroth, P. *J. Phys.: Condens. Matter* **2010**, *22*, 133001.
(11) Gonzalez, M. T.; Wu, S. M.; Huber, R.; van der Molen, S. J.; Schonenberger, C.; Calame, M. *Nano Lett.* **2006**, *6*, 2238−2242.
(12) Kamenetska, M.; Quek, S. Y.; Whalley, A. C.; Steigerwald, M. L.; Choi, H. J.; Louie, S. G.; Nuckolls, C.; Hybertsen, M. S.; Neaton, J. B.; Venkataraman, L. *J. Am. Chem. Soc.* **2010**, *132*, 6817−6821.
(13) Xing, Y. J.; Park, T. H.; Venkatramani, R.; Keinan, S.; Beratan, D. N.; Therien, M. J.; Borguet, E. *J. Am. Chem. Soc.* **2010**, *132*, 7946−7956.
(14) Chen, F.; Tao, N. J. *Acc. Chem. Res.* **2009**, *42*, 573−573.
(15) Tivanski, A. V.; He, Y. F.; Borguet, E.; Liu, H. Y.; Walker, G. C.; Waldeck, D. H. *J. Phys. Chem. B* **2005**, *109*, 5398−5402.
(16) Qian, G. G.; Saha, S.; Lewis, K. M. *Appl. Phys. Lett.* **2010**, *96*, 243107.
(17) Huang, Z. F.; Chen, F.; Bennett, P. A.; Tao, N. J. *J. Am. Chem. Soc.* **2007**, *129*, 13225−13231.
(18) Kiguchi, M.; Takahashi, T.; Kanehara, M.; Teranishi, T.; Murakoshi, K. *J. Phys. Chem. C* **2009**, *113*, 9014−9017.
(19) Li, Z. H.; Pobelov, I.; Han, B.; Wandlowski, T.; Blaszczyk, A.; Mayor, M. *Nanotechnology* **2007**, *18*, 044018.
(20) Venkataraman, L.; Klare, J. E.; Nuckolls, C.; Hybertsen, M. S.; Steigerwald, M. L. *Nature* **2006**, *442*, 904−907.
(21) Dell'Angela, M.; Kladnik, G.; Cossaro, A.; Verdini, A.; Kamenetska, M.; Tamblyn, I.; Quek, S. Y.; Neaton, J. B.; Cvetko, D.; Morgante, A.; Venkataraman, L. *Nano Lett.* **2010**, *10*, 2470−2474.
(22) Lortscher, E.; Cho, C. J.; Mayor, M.; Tschudy, M.; Rettner, C.; Riel, H. *Chemphyschem* **2011**, *12*, 1677−1682.

(23) Tam, E. S.; Parks, J. J.; Shum, W. W.; Zhong, Y. W.; Santiago-Berrios, M. B.; Zheng, X.; Yang, W. T.; Chan, G. K. L.; Abruna, H. D.; Ralph, D. C. *ACS Nano* **2011**, *5*, 5115−5123.
(24) He, Y.; Borguet, E. *Angew. Chem., Int. Ed.* **2007**, *46*, 6098−6101.
(25) Yuan, Q. H.; Xing, Y. J.; Borguet, E. *J. Am. Chem. Soc.* **2010**, *132*, 5054−5060.
(26) Li, Z.; Han, B.; Meszaros, G.; Pobelov, I.; Wandlowski, T.; Blaszczyk, A.; Mayor, M. *Faraday Discuss.* **2006**, *131*, 121−143.
(27) Li, X. L.; He, J.; Hihath, J.; Xu, B. Q.; Lindsay, S. M.; Tao, N. J. *J. Am. Chem. Soc.* **2006**, *128*, 2135−2141.